

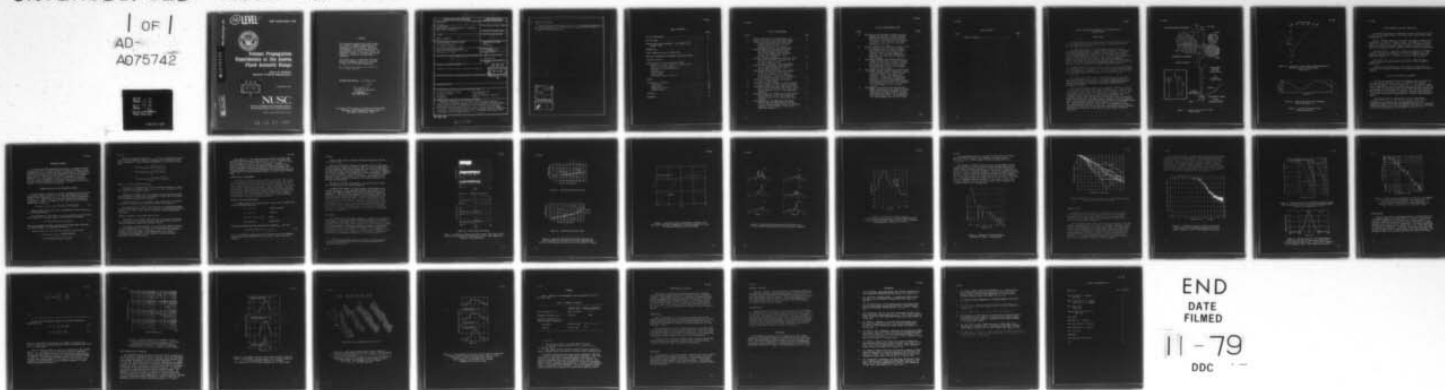
AD-A075 742

NAVAL UNDERWATER SYSTEMS CENTER NEW LONDON CT NEW LO--ETC F/G 17/1
VOLUME PROPAGATION EXPERIMENTS AT THE AZORES FIXED ACOUSTIC RAN--ETC(U)
SEP 79 B G BUEHLER
NUSC-TR-5785

UNCLASSIFIED

1 OF 1
AD-A075742

NL



NUSC Technical Report 5785

(12) LEVEL II

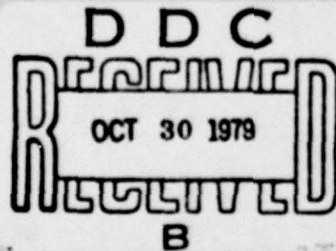
NUSC Technical Report 5785



Volume Propagation Experiments at the Azores Fixed Acoustic Range

Barry G. Buehler
Special Projects Department

AD A 075742



21 September 1979

NUSC

NAVAL UNDERWATER SYSTEMS CENTER
Newport, Rhode Island • New London, Connecticut

Approved for public release; distribution unlimited.

DDC FILE COPY

79 10 29 121

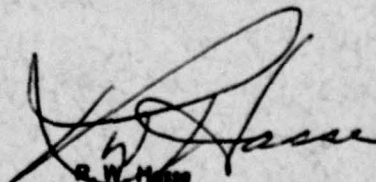
PREFACE

This report was prepared under NUSC Project No. A-600-00, "Acoustic Communications for Submarines and Sonar Vessels," Principal Investigator, A. W. Ellinthorpe (Code 3103), and Subproject and Task No. S2318-16180. The sponsoring activity is the Naval Sea Systems Command, J. Calabrese, Program Manager (SEA-661E).

The author wishes to acknowledge and thank Alan W. Ellinthorpe, Senior U.S. Scientist at AFAR, for his valuable suggestions.

The Technical Reviewer for this report was Dr. P. Cable (Code 313).

REVIEWED AND APPROVED: 21 September 1979


R. W. Hesse
Special Projects Department

The author of this report is located at the New London Laboratory, Naval Underwater Systems Center, New London, Connecticut 06320

141 NUSC-TR-5785

REPORT DOCUMENTATION PAGE		READ INSTRUCTIONS BEFORE COMPLETING FORM
1. REPORT NUMBER TR 5785	2. GOVT ACCESSION NO.	3. RECIPIENT'S CATALOG NUMBER
4. TITLE (and Subtitle) VOLUME PROPAGATION EXPERIMENTS AT THE AZORES FIXED ACOUSTIC RANGE		5. TYPE OF REPORT & PERIOD COVERED
7. AUTHOR(s) BARRY G. BUEHLER		6. PERFORMING ORG. REPORT NUMBER
9. PERFORMING ORGANIZATION NAME AND ADDRESS Naval Underwater Systems Center New London Laboratory New London, Connecticut 06320		8. CONTRACT OR GRANT NUMBER(s) 12371
11. CONTROLLING OFFICE NAME AND ADDRESS Naval Sea Systems Command (SEA-661E) Washington, DC 20362		10. PROGRAM ELEMENT, PROJECT, TASK AREA & WORK UNIT NUMBERS A60000 S2318-16180
12. MONITORING AGENCY NAME & ADDRESS (if different from Controlling Office) 16 S2318 17 S2318		11. REPORT DATE 21 September 1979
13. DISTRIBUTION STATEMENT (of this Report) Approved for public release; distribution unlimited.		12. NUMBER OF PAGES 33
14. DISTRIBUTION STATEMENT (of the abstract entered in Block 20, if different from Report)		13. SECURITY CLASS. (of this report) UNCLASSIFIED
15. SUPPLEMENTARY NOTES		14. DECLASSIFICATION/DOWNGRADING SCHEDULE
16. KEY WORDS (Continue on reverse side if necessary and identify by block number) Azores Fixed Acoustic Range Time, Frequency, and Covariance Lengths Space Domains Micropaths Volume Only (Direct) Acoustic Propagation Paths		
17. ABSTRACT (Continue on reverse side if necessary and identify by block number) Acoustic propagation over two purely refracted undersea paths is characterized by coherence lengths in the time, frequency, and space domains. Intensity fluctuations are quantified by the variance of log intensity. Measurements have been carried out on 1.5 and 18 nmi paths at the Azores Fixed Acoustic Range (AFAR) over the decade of acoustic frequencies from 500 to 5000 Hz. The 18 nmi path breaks up into "micropaths" resulting in self-interference of the deterministic ray. → over		

DDC
RECEIVED
OCT 30 1979
B

405918

JOB

20. ABSTRACT (Continued)

The long experiment averaging times, onsite oceanographic measurements, and repeatability of results make the results useful in the evaluation of acoustic propagation models.

ACCESSION for		
NTIS	White Section	<input checked="" type="checkbox"/>
DDC	Buff Section	<input type="checkbox"/>
UNANNOUNCED		<input type="checkbox"/>
JUSTIFICATION		
BY		
DISTRIBUTION/AVAILABILITY CODES		
Dist.	AVAIL	and/or SPECIAL
A		

TABLE OF CONTENTS

	Page
LIST OF ILLUSTRATIONS	ii
LIST OF TABLES	iv
VOLUME PROPAGATION EXPERIMENTS AT THE AZORES FIXED ACOUSTIC RANGE	1
INTRODUCTION	1
SIGNAL GENERATION AND DATA ACQUISITION	4
THE JOINT OCEANOGRAPHIC EXPERIMENT PROPAGATION MODELS	4
PROPAGATION MODELS	5
CHARACTERIZATION OF THE PROPAGATION CHANNEL	5
Temporal Isolation of the Direct Acoustic Path	6
Extraction of A/CW Estimate	7
Intensity and Phase Measurements	7
Time Smear	8
Frequency Smear	15
Angular Smear	18
Time Lagged Spatial Covariance	20
SUMMARY	24
EXTRAPOLATION OF RESULTS	25
Steeper Rays	25
Deeper Rays	25
Geographic Position	26
Platform Motion	26
CONCLUSION	26
REFERENCES	27

LIST OF ILLUSTRATIONS

Figure		Page
1	Overall Front View of an AFAR Antenna Tower	2
2	Direct Path Ray Trace and Sound Speed Profile	3
3	Intensity and Phase Delay Time Series, AFAR 18-nmi Direct Path (130 ms Gaussian Envelope Pulses, 10.158 s Pulse Repetition Interval), CW Approximation	9
4	Empirical Amplitude Distribution Functions for AFAR Unsaturated and Saturated Direct Paths Compared With Log Normal and Rayleigh Distributions (Plot Courtesy H. A. Freese)	10
5	Variance of Natural Logarithm of Intensity From AFAR Direct Path Data (Frequency (f) in Hz, Path Length (L) in m). 95 Percent Confidence Limits Are Shown	11
6	Received Pulse Envelopes at 5 min Separations (1.25 ms Gaussian Envelope Pulses at 3200 Hz Center Frequency)	12
7	Time Spread Indicating the Incoherent Average of 140 hr of Pulses Received Over the 18-nmi Direct Path (1.25 ms Gaussian Envelope Pulses, 3200 Hz Center Frequency, Pulse Repetition Interval of 10.158 s)	13
8	Frequency Covariance Estimate (Transform of Figure 7, Time Spread)	14
9	Frequency Covariance Estimates at Eight Different Center Frequencies, AFAR 18-nmi Direct Path . . .	15
10	Differential Doppler Estimate, AFAR 18-nmi Direct Path (130 ms Gaussian Envelope Pulses, 412 Hz Center Frequency, 10.158 s Pulse Repetition Interval)	16
11	Smoothed Estimates of Differential Doppler Spread, AFAR 18-nmi Direct Path (130 ms Gaussian Envelope Pulses, 10.158 s Pulse Repetition Interval)	17
12	Autocovariance of a CW (Approximation) Signal Received Over the AFAR 18-nmi Direct Path (130 ms Gaussian Envelope Pulses, 412 Hz Center Frequency, 110 hr Average, 10.158 s Pulse Repetition Interval)	17

LIST OF ILLUSTRATIONS (CONT)

Figure		Page
13	Time Lag for Autocovariance to Decay to $1/e$ of Maximum as a Function of Center Frequency; AFAR 18-nmi Direct Path (130 ms Gaussian Envelope Pulses, Pulse Repetition Intervals < 10.158 s). Solid Line is a Least Mean Squares Fit, $\tau_{1/e} = CF$; $C = 9.2 \times 10^5$, $\alpha = -1.12 \pm \sigma$, $\sigma = 0.06$	18
14	Spatial Separation for Covariance to Decay to $1/e$ as a Function of Pulse Center Frequency. AFAR 18-nmi Direct Path (130 ms Gaussian Envelope Pulses, 3 s Pulse Repetition Interval). The Horizontal Separation is Shown With Dots, the Vertical Separation With Triangles	20
15	Time Lagged Crosscovariance Between Spatially Separated Antenna (130 ms Gaussian Envelope Pulses, 4671 Hz Center Frequency, 10.158 s Pulse Repetition Interval, 6 hr Average). The Antenna Pairs Lie in a Plane Perpendicular to Line of Sight	21
16	Time Lagged Crosscovariance Between Antenna Pairs at the Indicated Spatial Separations (130 ms Gaussian Envelope Pulses, 4671 Hz Center Frequency, 10.158 s Pulse Repetition Interval). ΔX Represents the Horizontal Separation, ΔY the Vertical Separation. Each Group Contains 14 Covariance Estimates From Contiguous Time Blocks. Each Estimate is a 6-hr Average ($6 \times 14 = 84$ Total Data hr)	22
17	Time Lagged Crosscovariance Between Spatially Separated Antennas (130 ms Gaussian Envelope Pulses, 4671 Hz Center Frequency, 10.158 s Pulse Repetition Interval, 84 hr Averages), AFAR 18-nmi Direct Path. The Antennas are in a Plane Perpendicular to Line of Sight	23

LIST OF TABLES

Table		Page
1	Summary of Results	24
2	Summary of Results	25
3	Summary of Results	26
4	Summary of Results	27
5	Summary of Results	28
6	Summary of Results	29
7	Summary of Results	30
8	Summary of Results	31
9	Summary of Results	32
10	Summary of Results	33
11	Summary of Results	34
12	Summary of Results	35
13	Summary of Results	36
14	Summary of Results	37
15	Summary of Results	38
16	Summary of Results	39
17	Summary of Results	40
18	Summary of Results	41
19	Summary of Results	42
20	Summary of Results	43
21	Summary of Results	44
22	Summary of Results	45
23	Summary of Results	46
24	Summary of Results	47
25	Summary of Results	48
26	Summary of Results	49
27	Summary of Results	50
28	Summary of Results	51
29	Summary of Results	52
30	Summary of Results	53
31	Summary of Results	54
32	Summary of Results	55
33	Summary of Results	56
34	Summary of Results	57
35	Summary of Results	58
36	Summary of Results	59
37	Summary of Results	60
38	Summary of Results	61
39	Summary of Results	62
40	Summary of Results	63
41	Summary of Results	64
42	Summary of Results	65
43	Summary of Results	66
44	Summary of Results	67
45	Summary of Results	68
46	Summary of Results	69
47	Summary of Results	70
48	Summary of Results	71
49	Summary of Results	72
50	Summary of Results	73
51	Summary of Results	74
52	Summary of Results	75
53	Summary of Results	76
54	Summary of Results	77
55	Summary of Results	78
56	Summary of Results	79
57	Summary of Results	80
58	Summary of Results	81
59	Summary of Results	82
60	Summary of Results	83
61	Summary of Results	84
62	Summary of Results	85
63	Summary of Results	86
64	Summary of Results	87
65	Summary of Results	88
66	Summary of Results	89
67	Summary of Results	90
68	Summary of Results	91
69	Summary of Results	92
70	Summary of Results	93
71	Summary of Results	94
72	Summary of Results	95
73	Summary of Results	96
74	Summary of Results	97
75	Summary of Results	98
76	Summary of Results	99
77	Summary of Results	100

VOLUME PROPAGATION EXPERIMENTS AT THE AZORES FIXED ACOSUTIC RANGE

INTRODUCTION

The Azores Fixed Acoustic Range (AFAR) was an international research and development project in underwater acoustics in which eight member nations of NATO participated.¹

The range consisted of a transmitting/receiving array mounted 30 m above the ocean bottom at a depth of 540 m (figure 1), two similarly constructed receiving arrays at depths of 256 and 736 m, and an omnidirectional hydrophone at a depth of 325 m. The three array positions formed an almost equilateral triangle 18 nmi on a side. The hydrophone was located 1.5 nmi from the source array. Each array was located on a mountain top plateau and the valley depth between these terminals reached 2500 m. The arrays were steerable in azimuth and elevation, and spanned the decade of acoustic frequencies from approximately 500 to 5000 Hz.

During the first half of the 1970's, a variety of acoustic experiments were performed at AFAR to measure the effects of the ocean surface, bottom, and volume on acoustic propagation in a bistatic situation. The published results of these experiments are summarized in "The AFAR Project - A Valediction."²

This report deals with a series of measurements carried out over volume-only (direct) acoustic paths. The ocean volume is common to all paths between source and receiver and its effect on propagation must be measured and understood if we hope to understand undersea acoustic propagation in general.

There were two direct acoustic paths available at AFAR that could be isolated in the time domain from boundary reflected paths. Figure 2 shows a ray tracing of the 18 nmi direct path linking the source array and the southernmost receiving array. The direct ray was confined to the range of depths from 400 to 800 m and to ray angles (referenced to the horizontal) under 2 deg. The existence of this path is due to a positive "hump" in the vertical sound speed profile, centered at a depth of approximately 1000 m, possibly caused by an intrusive outflow from the Mediterranean Sea. The second direct path at AFAR was between the source array and the omnidirectional hydrophone 1.5 nmi away. The experimental results presented below show that the two paths and the available acoustic frequency range allow investigation of both weak and strong scatter propagation conditions.

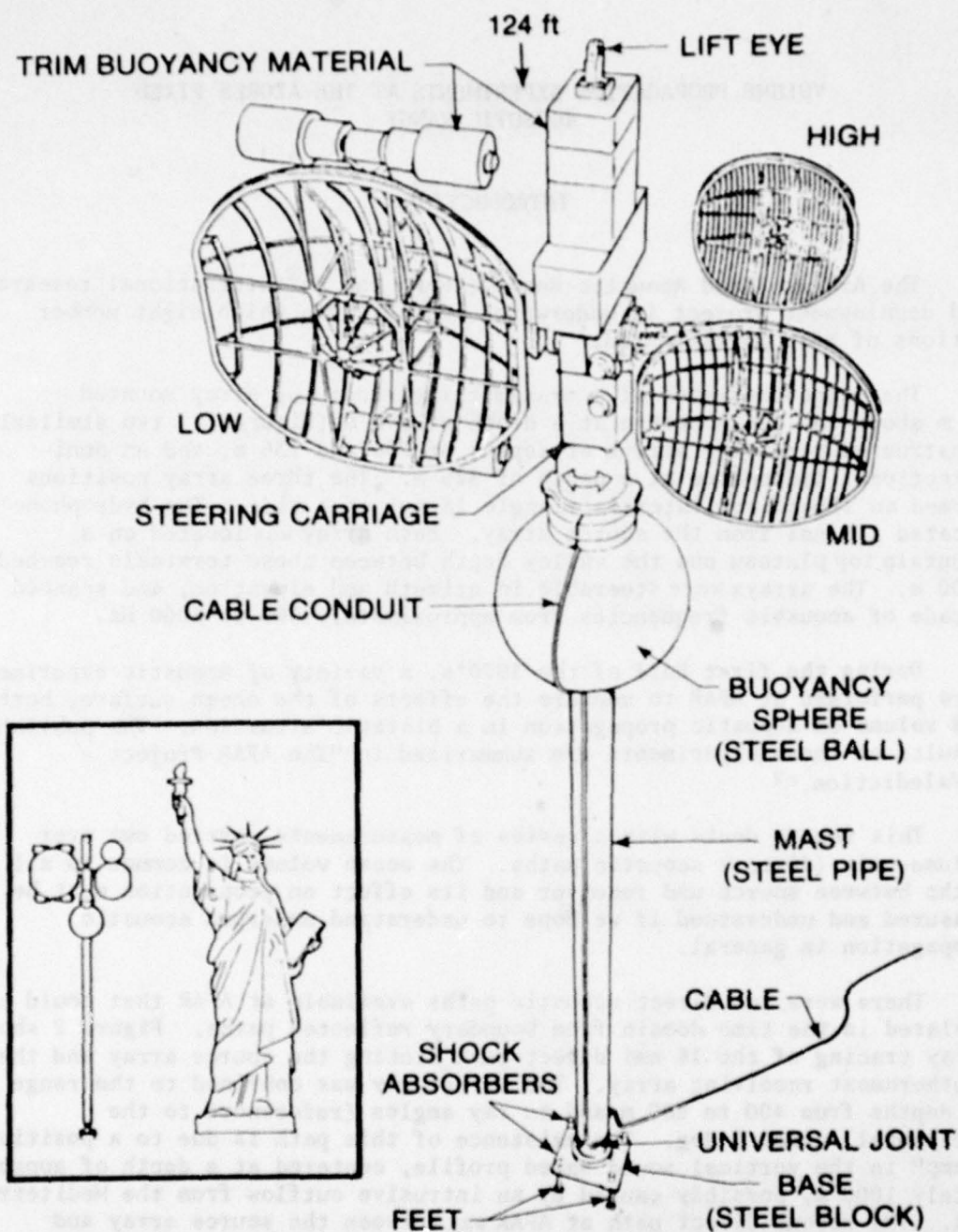


Figure 1. Overall Front View of an AFAR Antenna Tower

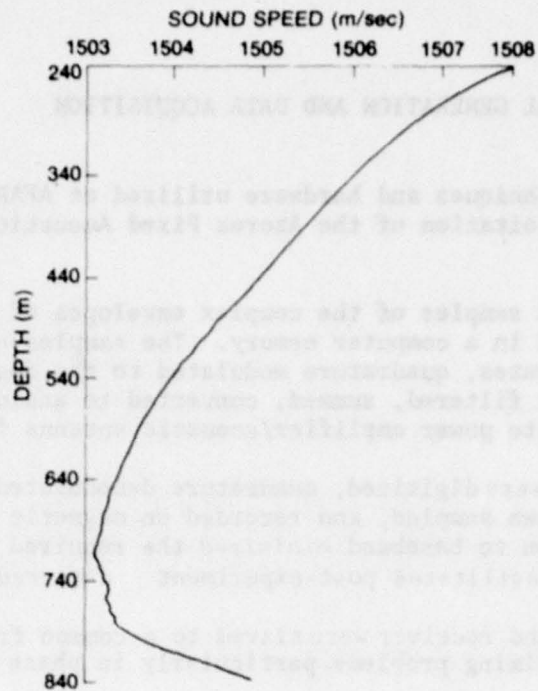


Figure 2a. Average of 57 Sound Speed Profiles Measured at AFAR During March 1975 Experiments (upper 840 m)

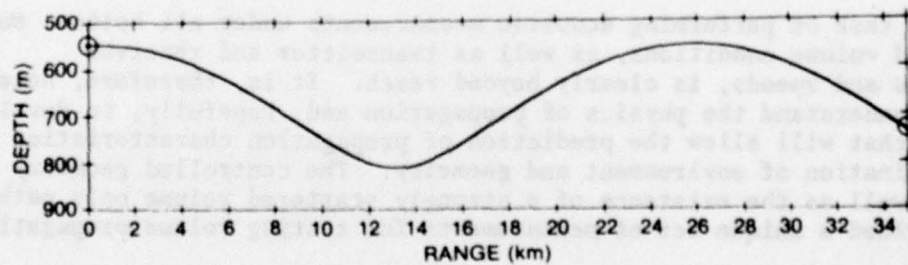


Figure 2b. AFAR 18-nmi Direct Ray From Speed Profile of Figure 2a

Figure 2. Direct Path Ray Trace and Sound Speed Profile

SIGNAL GENERATION AND DATA ACQUISITION

The signaling techniques and hardware utilized at AFAR are described in detail in the "Exploitation of the Azores Fixed Acoustic Range (AFAR) through May 1973."³

Briefly, baseband samples of the complex envelopes of signals to be transmitted were stored in a computer memory. The samples were read from memory at selectable rates, quadrature modulated to the desired center frequencies, digitally filtered, summed, converted to analog, and distributed to the appropriate power amplifier/acoustic antenna for transmission.

Received signals were digitized, quadrature demodulated to baseband, digitally filtered, down sampled, and recorded on magnetic tape. The quadrature demodulation to baseband minimized the required recording sample rate and also facilitated post-experiment data reduction.

The transmitter and receiver were slaved to a common frequency standard, eliminating timing problems, particularly in phase dependent computations.

Reference to data reduction in this report will assume that all operations are performed on samples of the complex envelopes of received signals.

THE JOINT OCEANOGRAPHIC EXPERIMENT

The task of performing acoustic measurements under all bottom, surface, and volume conditions, as well as transmitter and receiver positions and speeds, is clearly beyond reach. It is, therefore, necessary to understand the physics of propagation and, hopefully, to develop a model that will allow the prediction of propagation characteristics for any combination of environment and geometry. The controlled geometry at AFAR, as well as the existence of a strongly scattered volume only path, has provided a unique set of measurements for testing volume propagation models.

During March 1975, an international acoustic-oceanographic experiment was conducted at AFAR to obtain simultaneous, detailed environmental and acoustic data, and subsequently predict the propagation conditions from the environmental conditions.⁴⁻¹⁰ Individual results presented in this report are primarily from the March 1975 operation and are representative of other AFAR experimental results.

PROPAGATION MODELS

At the time the AFAR measurements were made, no propagation models (of which the author is aware) existed for strong scattering by random inhomogeneities in the ocean volume that simultaneously incorporated the effects of anisotropy, statistical inhomogeneity, and the deterministic sound channel.¹¹ Recent work, primarily by a subgroup of the JASON Committee,¹² has had remarkable success in predicting the measured acoustics using oceanographic data obtained during these experiments. The model includes the effects of anisotropy, inhomogeneity, and a sound channel, as well as internal wave spectra.

CHARACTERIZATION OF THE PROPAGATION CHANNEL

We have chosen to quantify the acoustic propagation characteristics of the ocean volume in terms of the second order statistics of its response to a sine wave excitation, i.e., the time varying transfer function $H(f, t, r)$. When $H(f, t, r)$ is wide sense stationary in the three variables of t (time), f (frequency), and r (space), we can write the second order statistic as

$$R(t_1 - t_2, f_1 - f_2, r_1 - r_2) = \overline{H(t_1, f_1, r_1) H^*(t_2, f_2, r_2)} . \quad (1)$$

When we suppress the mean values in computation, we will refer to R as a covariance function.

The assumption of stationarity can not be justified a priori for the ocean volume. We, therefore, make a less restrictive assumption

$$R = R(t_1 - t_2, f_1 - f_2, r_1 - r_2, t_0, f_0, r_0) , \quad (2)$$

where R is assumed stationary over some narrow region about the epoch, t_0 , center frequency, f_0 , and spatial point, r_0 .

Finally, using τ , η , and S as shift variables, we can write

$$R(\tau, \eta, S; t_0, f_0, r_0) = \overline{H(t_0 + \tau/2, f_0 + \eta/2, r_0 + S/2) H^*(t_0 - \tau/2, f_0 - \eta/2, r_0 - S/2)} . \quad (3)$$

While the correlation function $R(\cdot)$ is useful in quantifying a propagation channel's effect on signals, the physics of the channel are most easily understood in terms of Fourier transforms of R on each shift variable.

$$R(\tau, 0, 0; t_0, f_0, r_0) \stackrel{\tau}{\leftrightarrow} \overline{A^2(\sigma; t_0, f_0, r_0)}$$

$$R(0, \eta, 0; t_0, f_0, r_0) \stackrel{\eta}{\leftrightarrow} \overline{h^2(\zeta; t_0, f_0, r_0)}$$

$$R(0, 0, s; t_0, f_0, r_0) \stackrel{s}{\leftrightarrow} \overline{s^2(\sin \alpha; t_0, f_0, r_0)},$$

$\sin \alpha$

where σ , ζ , and α are smear variables.

The extent of (nonnegligible) $\overline{A^2}$ (the differential Doppler spectrum) in σ represents the frequency smear imposed on a tone transmitted at $f=f_0$ by motions in the propagation medium.

Similarly, the extent of $\overline{h^2}$ in ζ measures the range of delays (time smear) imposed on a signal due to the different travel times of the paths connecting source and receiver (multipath).

The extent of $\overline{S^2}$ in α is the angular smear imposed on a transmitted plane wave by refractive and diffractive effects in the medium.

The functions $\overline{A^2}$, $\overline{h^2}$, and $\overline{S^2}$ can be measured by transmitting signals that are narrow compared with the imposed smears, corresponding effectively to impulses in time (a narrow pulse), frequency (a tone), and angle (a plane wave).

TEMPORAL ISOLATION OF THE DIRECT ACOUSTIC PATH

Measurement of the second order statistics of the transfer function $R(\tau, \eta, s; t_0, f_0, r_0)$ for the direct acoustic path necessitates isolation of that path from other significant multipath arrivals.

Fortunately, the time occupancy of the direct path impulse response was small compared with its isolation in time from nondirect arrivals. (This is true for both the 18 and 1.5 nmi paths.) This made it possible to transmit pulses long enough to allow measurement of the direct path steady state response but short enough to prevent intersymbol interference from nondirect paths.

Measurement of R also requires pulse repetition intervals small compared to the direct path correlation time. It will be shown below that the repetition intervals used at AFAR (typically 3 and 10 s) yielded smooth estimates of the time covariance function. Although it is possible to contrive time varying transfer functions that will yield smooth, repeatable covariance estimates even when undersampled, the stochastic nature of ocean volume propagation allows the conclusion that sample rates > 0.1 Hz are sufficiently high at all AFAR acoustic frequencies.

EXTRACTION OF A CW ESTIMATE

Sequences of narrowband Gaussian envelope pulses were used to simulate CW transmission over the AFAR direct acoustic paths. The received pulse intensities were computed as time functions extending over each pulse repetition interval and were then averaged to determine the average channel power response over the duration of each experiment. The transmission delay of the peak average power response was determined and the individual received waveforms were sampled (tapped) at that fixed transmission delay. The resulting sample sequence approximates sampling a CW transmission over an isolated direct path using a uniform sampling interval equal to the pulse repetition interval.

INTENSITY AND PHASE MEASUREMENTS

The tapped sequences of quadrature data s_i were used to compute time series of intensity and phase:

$$s_i = U_i + jV_i \quad \text{complex envelope}$$

$$I_i = U_i^2 + V_i^2 \quad \text{intensity}$$

$$\phi_i = \tan^{-1} V_i/U_i + N_i 2\pi \quad \text{phase}$$

$$T_i = \phi_i / (2\pi f_0) \quad \text{phase delay.}$$

Time series of phase are made continuous by finding N_{i+1} , such that

$$|\phi_{i+1} + (N_{i+1} - N_i) 2\pi - \phi_i| \leq \pi; N_0 = 0. \quad (4)$$

This is justified by assuming that phase variations are due to smoothly varying pulse arrival times and $(\phi_{i+1} - \phi_i) / 2\pi f_0 \ll$ pulse repetition interval.

Figure 3 shows typical intensity and phase delay plots for the 18 nmi direct path.

Empirical distribution functions of envelope level $|S_i|$ were computed, and typical results are shown in figure 4. At short range and low acoustic frequency (weak scatter regime), the statistics are log normal as predicted by first order perturbation theory.¹¹ As acoustic frequency and range are increased, the deterministic direct path begins to break up into a tube of randomly varying "micropaths."¹² At sufficiently high frequencies (and/or long ranges), the micropaths add randomly at the receiver, yielding quadrature components with Gaussian statistics (a Rayleigh fading envelope).

The AFAR 1.5 nmi data are apparently log normal and the 18 nmi data are Rayleigh* at all center frequencies.

A commonly used measure of signal intensity fluctuation is the variance of $\log(I)$. First order perturbation theory predicts a log variance that increases monotonically with both range and acoustic frequency.¹⁰ This is clearly a nonphysical result and, in fact, the variation in log intensity saturates at a level corresponding to the value predicted for Rayleigh fading. Figure 5 shows values of log variance computed using AFAR direct path data. The abscissa scaling is that which will yield a linear dependence predicted by first order perturbation theory.¹¹ Data in the saturated regime (Rayleigh limit) were obtained on the 18 nmi direct path, and data on the increasing portion of the curve were obtained from the 1.5 nmi path. The saturation curve is similar to those observed in atmospheric electromagnetic propagation measurements.

TIME SMEAR

The duration of the time smear imposed on a signal by a transmission channel can be directly measured by transmitting pulses of short duration compared to the smear. Figure 6 is a set of envelopes of direct path arrivals produced by 1.25 ms pulses transmitted at a center frequency of 3200 Hz. The multimodal arrival structure is spread over about a 10 ms transmission delay. Figure 7 is an incoherent average of 48000 consecutive pulse arrivals (a 140-hr average); i.e., figure 7 is an estimate of $\overline{h^2}(\xi)$. A theoretical average power response curve derived by the JASON group, using measured oceanographic parameters, is an excellent match.¹²

* The JASON work predicts that the statistics are not precisely Rayleigh and investigation of higher order intensity moments has verified this prediction.¹²

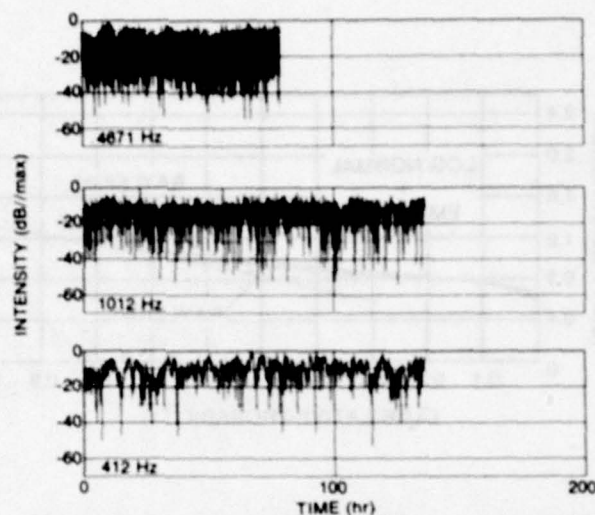


Figure 3a. Intensity Time Series

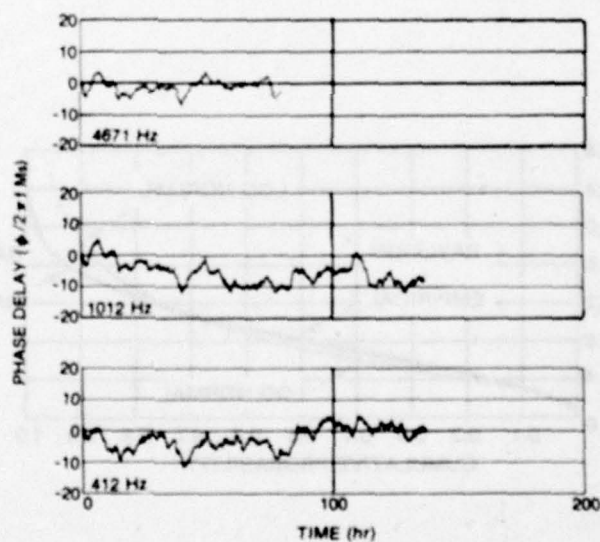


Figure 3b. Phase Delay Time Series

Figure 3. Intensity and Phase Delay Time Series, AFAR 18-nmi Direct Path (130 ms Gaussian Envelope Pulses, 10.158 s Pulse Repetition Interval), CW Approximation

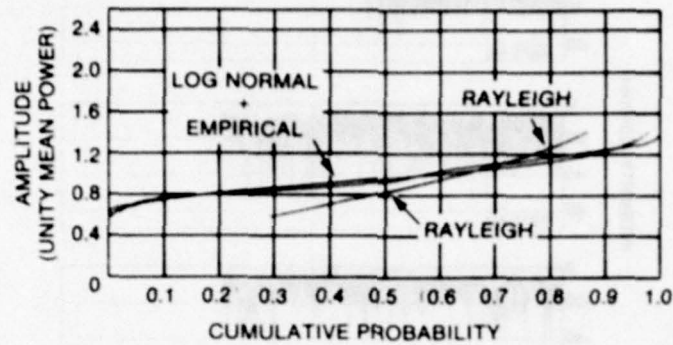


Figure 4a. AFAR Unsaturated Direct Path

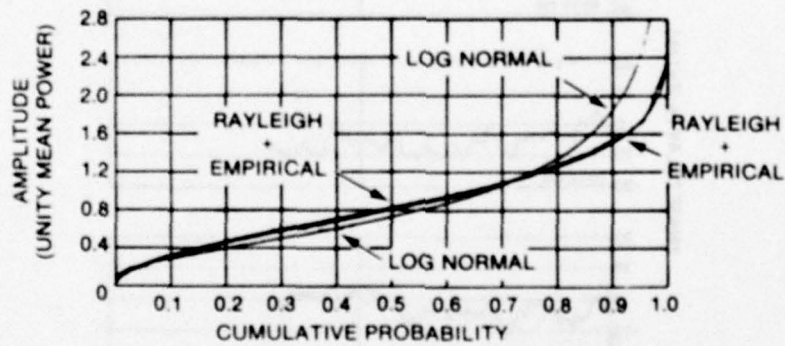


Figure 4b. AFAR Saturated Direct Path

Figure 4. Empirical Amplitude Distribution Functions for AFAR Unsaturated and Saturated Direct Paths Compared With Log Normal and Rayleigh Distributions (Plot Courtesy H.A. Freese)

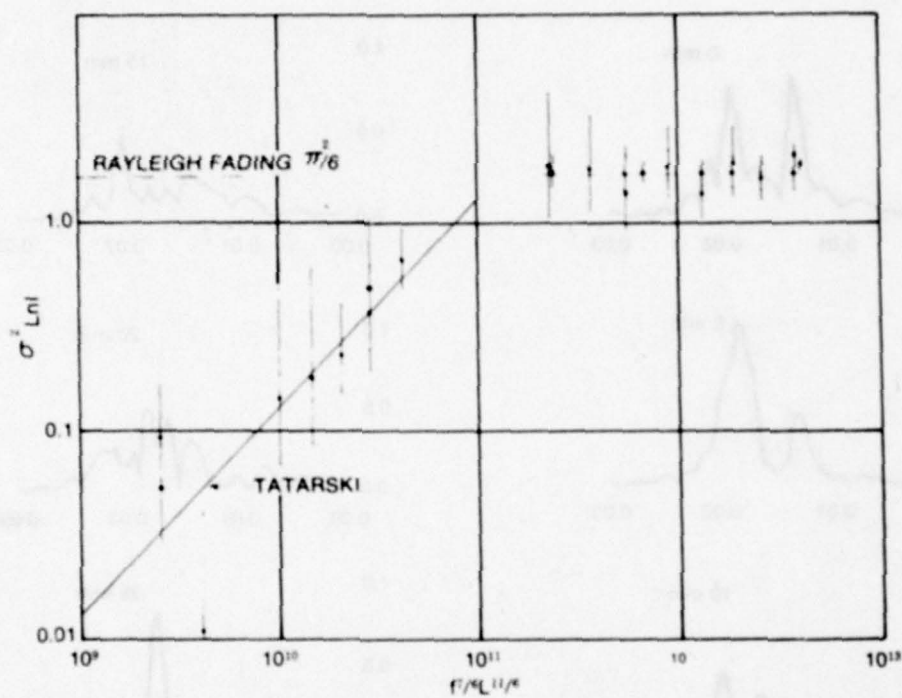


Figure 5. Variance of Natural Logarithm of Intensity From AFAR Direct Path Data (Frequency (f) in Hz, Path Length (L) in m). 95 Percent Confidence Limits Are Shown

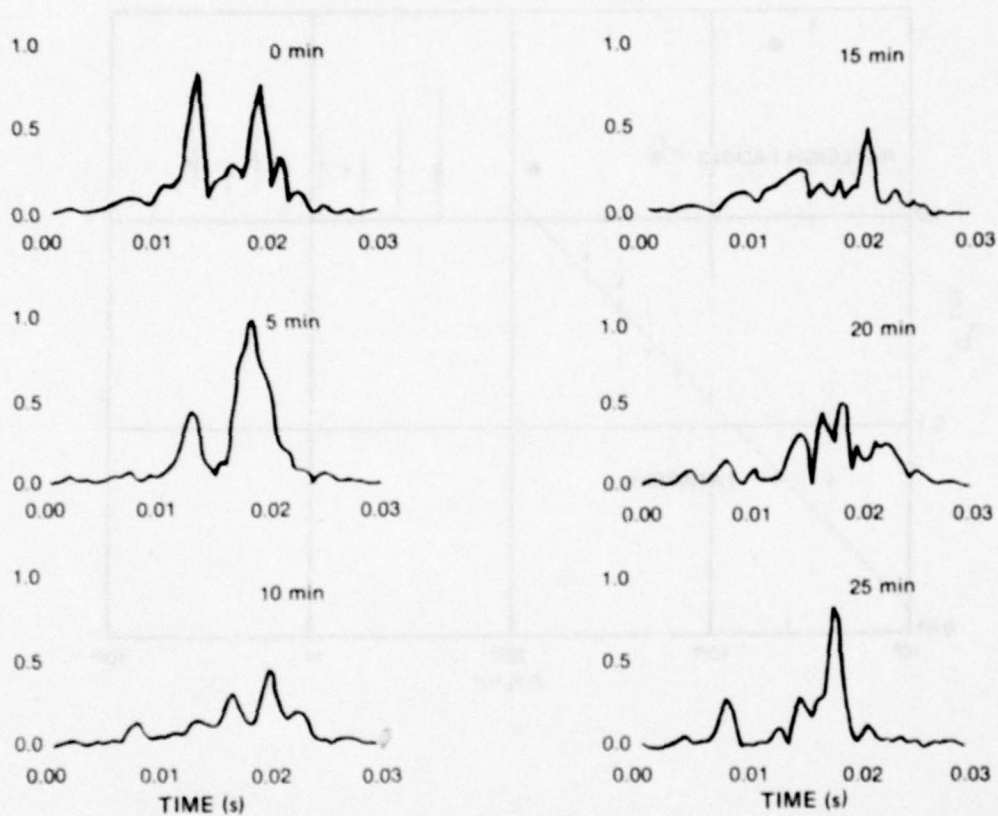


Figure 6. Received Pulse Envelopes at 5 min Separations
(1.25 ms Gaussian Envelope Pulses at 3200 Hz Center Frequency)

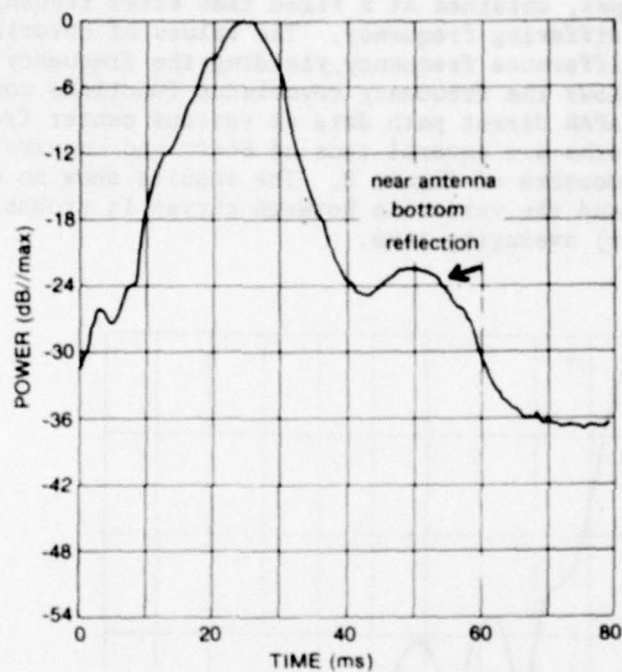


Figure 7. $\overline{h^2}(\xi)$, the Incoherent Average of 140 hr of Pulses Received Over the 18-nmi Direct Path (1.25 ms Gaussian Envelope Pulses, 3200 Hz Center Frequency, Pulse Repetition Interval of 10.158 s)

As was pointed out earlier, the Fourier transform of the channel time smear $h^*(\zeta; t_0, f_0, r_0)$ is the frequency covariance function $R(o, \eta, o; t_0, f_0, r_0)$. Figure 8 shows the Fourier transform of $h^*(\zeta)$ of figure 7.

The frequency covariance function can also be generated directly by computing the zero time lag crosscovariance between samples of the complex signal envelopes, obtained at a fixed time after transmission, of two CW signals of differing frequency. The values of covariance are then plotted versus difference frequency, yielding the frequency covariance function. Figure 9 shows the frequency covariance functions computed from several sets of AFAR direct path data at various center frequencies. The e^{-1} covariance widths are several tens of hertz and compare favorably with the independent measure of figure 8. The results show no clear frequency dependence, and the variation between curves is probably due to insufficient (10 hr) averaging time.

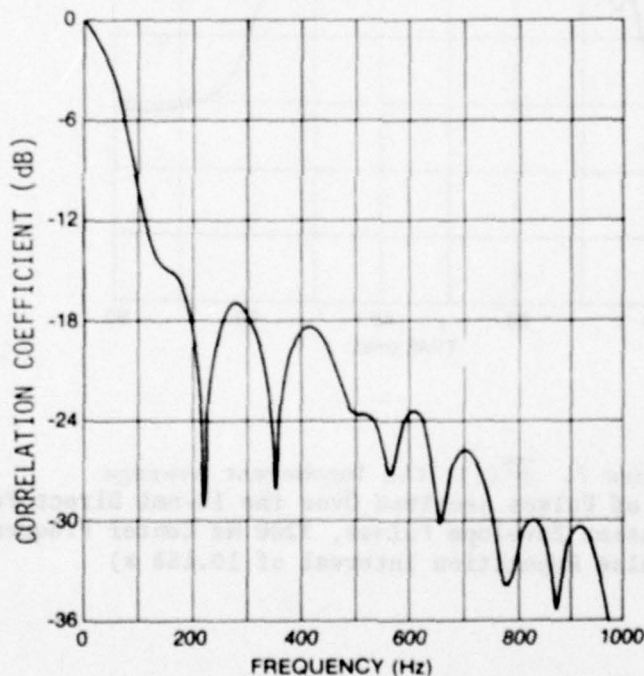


Figure 8. Frequency Covariance Estimate
(Transform of Figure 7, Time Spread)

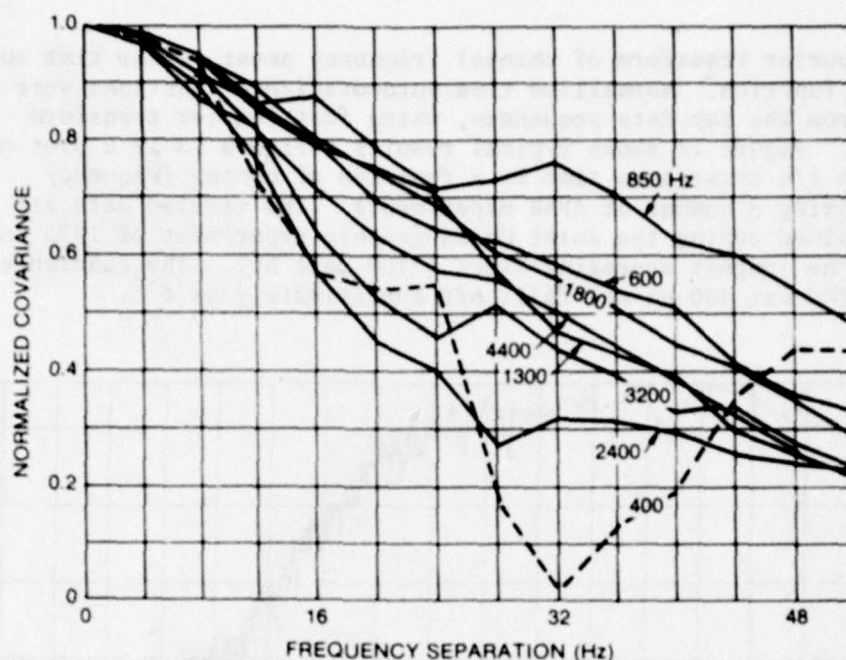


Figure 9. Frequency Covariance Estimates at Eight Different Center Frequencies, AFAR 18-nmi Direct Path

FREQUENCY SMEAR

Differential Doppler spectra have been computed for the 18 nmi direct acoustic path by transmitting sequences of 130 ms Gaussian envelope pulses of fixed center frequency. The pulse repetition interval of 10 s is small compared to the measured covariance times at all AFAR experimental frequencies.

The tap sequences were broken into 50 percent overlapped, zero mean segments, Hanning windowed, and Fourier transformed. Magnitude squared spectra were averaged over all segments and normalized to obtain power spectral density estimates. Figure 10 shows a typical result for the 18 nmi direct path obtained by averaging five 40 hr, 50 percent overlapped segments (120 data hr). Figure 11 contains smoothed spectral estimates for data taken simultaneously at three different center frequencies. The measured frequency smears are on the order of millihertz and, as expected, increase with center frequency.

The Fourier transform of channel frequency smear is the time autocovariance function. Normalized time autocovariance functions were computed from the tap data sequences, using fast Fourier transform techniques. Figure 12 shows typical results. Figure 13 is a plot of direct path 1/e covariance time as a function of center frequency measured during a number of AFAR experiments. The circled data are values obtained during the Joint Oceanographic Experiment of 1975 and represent the longest averaging times (≈ 100 data hr). The coherence time is ≈ 1000 s at 400 Hz and falls off approximately as f^{-1} .

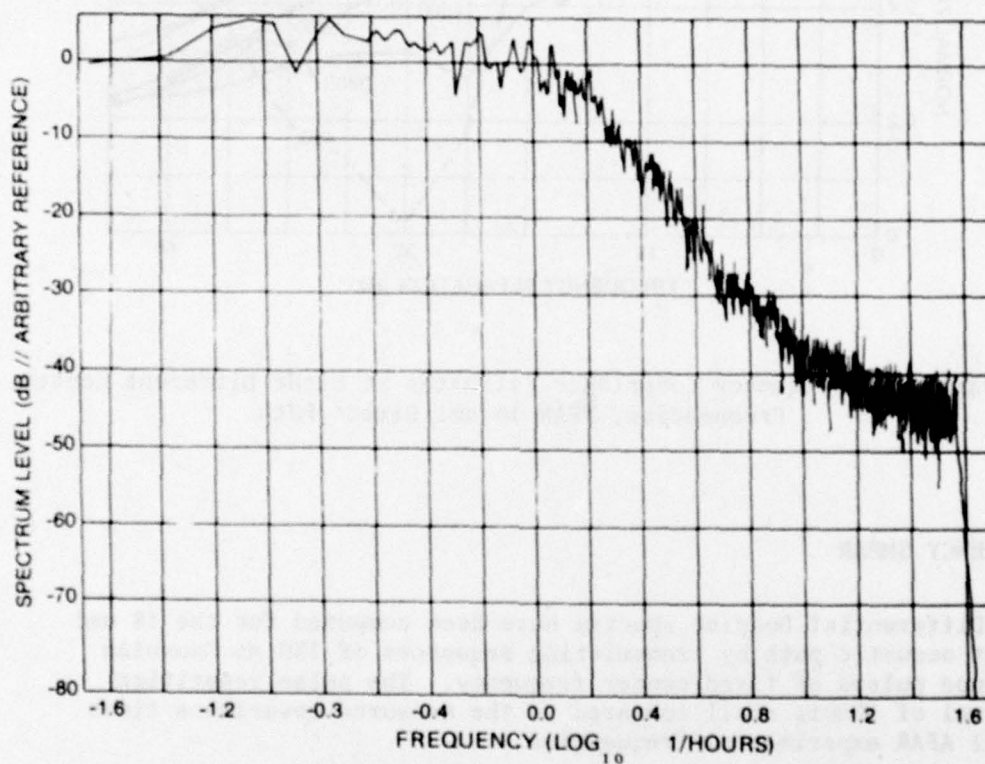


Figure 10. Differential Doppler Estimate, AFAR 18-nmi
Direct Path (130 ms Gaussian Envelope Pulse, 412 Hz
Center Frequency, 10.158 s Pulse Repetition Interval)

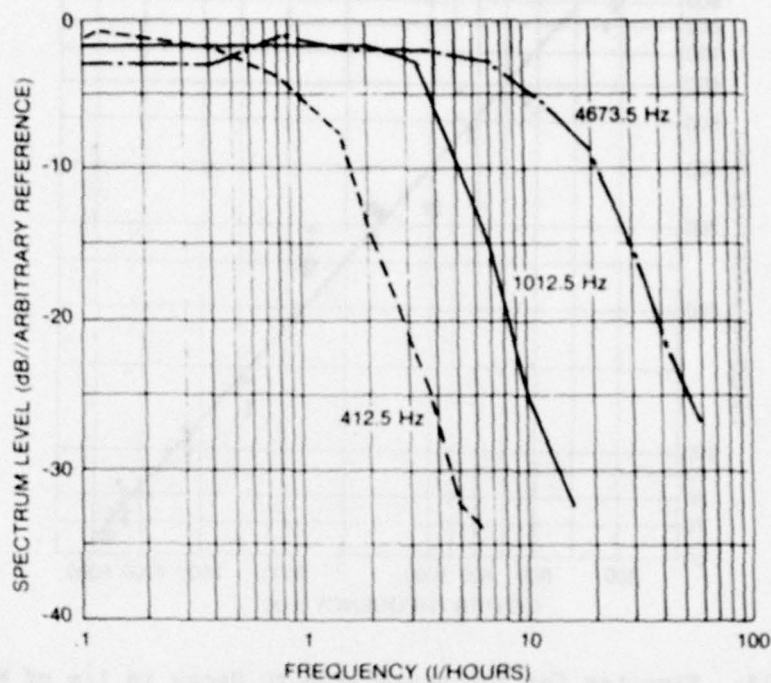


Figure 11. Smoothed Estimates of Differential Doppler Spread, AFAR 18-nmi Direct Path (130 ms Gaussian Envelope Pulses, 10.158 s Pulse Repetition Interval)

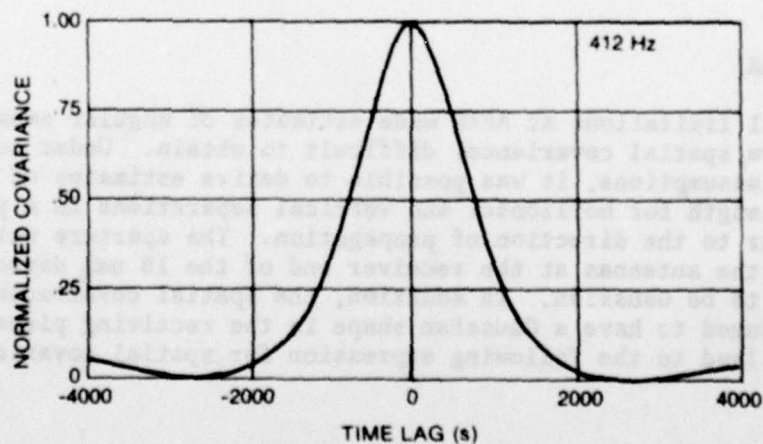


Figure 12. Autocovariance of a CW (Approximation) Signal Received Over the AFAR 18-nmi Direct Path (130 m Gaussian Envelope Pulses, 412 Hz Center Frequency, 110 hr Average, 10.158 s Pulse Repetition Interval)

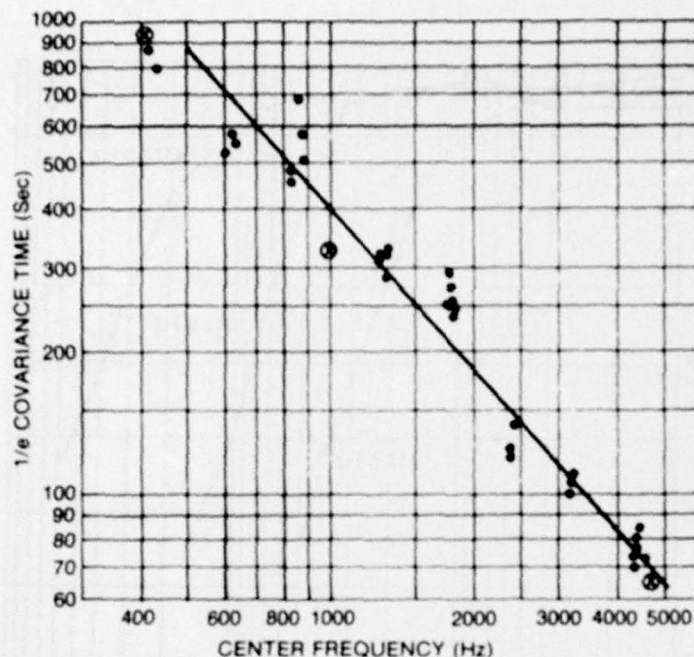


Figure 13. Time Lag for Autocovariance to Decay to 1/e of Maximum as a Function of Center Frequency, AFAR 18-nmi Direct Path (130 ms Gaussian Envelope Pulses, Pulse Repetition Intervals < 10.158 s). Solid Line is a Least Mean Square Fit, $\tau_{1/e} = CF^\alpha$; $C = 9.2 \times 10^5$, $\alpha = -1.12 \pm \sigma$, $\sigma = 0.06$.

ANGULAR SMEAR

Physical limitations at AFAR made estimates of angular smear (or its transform, spatial covariance) difficult to obtain. Under certain restrictive assumptions, it was possible to derive estimates of 1/e covariance length for horizontal and vertical separations in a plane perpendicular to the direction of propagation. The aperture weighting for each of the antennas at the receiver end of the 18 nmi direct path was assumed to be Gaussian. In addition, the spatial covariance function was assumed to have a Gaussian shape in the receiving plane. The assumptions lead to the following expression for spatial covariance:¹³

$$C = \frac{\alpha\beta}{AB} \exp \left\{ -\frac{X_0^2}{A^2} - \frac{Y_0^2}{B^2} \right\}, \quad (5)$$

where

X_0, Y_0 are the horizontal and vertical separation of the antenna pair,

α, β are the 1/e covariance lengths in the X and Y directions, respectively, and

$$A^2 = \alpha^2 + \mu_1^2 R_1^2 + \mu_2^2 R_2^2, \quad (6)$$

$$B^2 = \beta^2 + \mu_1^2 R_1^2 + \mu_2^2 R_2^2. \quad (7)$$

where R is the radius of the antenna (see figure 1), and μR is the effective radius of the antenna aperture at which the response has fallen to 1/e of the maximum.

Since the three antennas are similarly constructed, it was assumed that $\mu_1 = \mu_2$. Estimates of the horizontal and vertical covariance lengths (α, β) were computed using the three available antenna pairs at the receiver; the results are plotted as a function of center frequency in figure 14. The resulting covariance lengths ($\approx 60\lambda$ horizontal, $\approx 10\lambda$ vertical) imply angular smears $\approx 1^\circ$ horizontal and $\approx 5^\circ$ vertical. The asymmetry is a manifestation of a corresponding asymmetry in oceanic index of refraction variations.

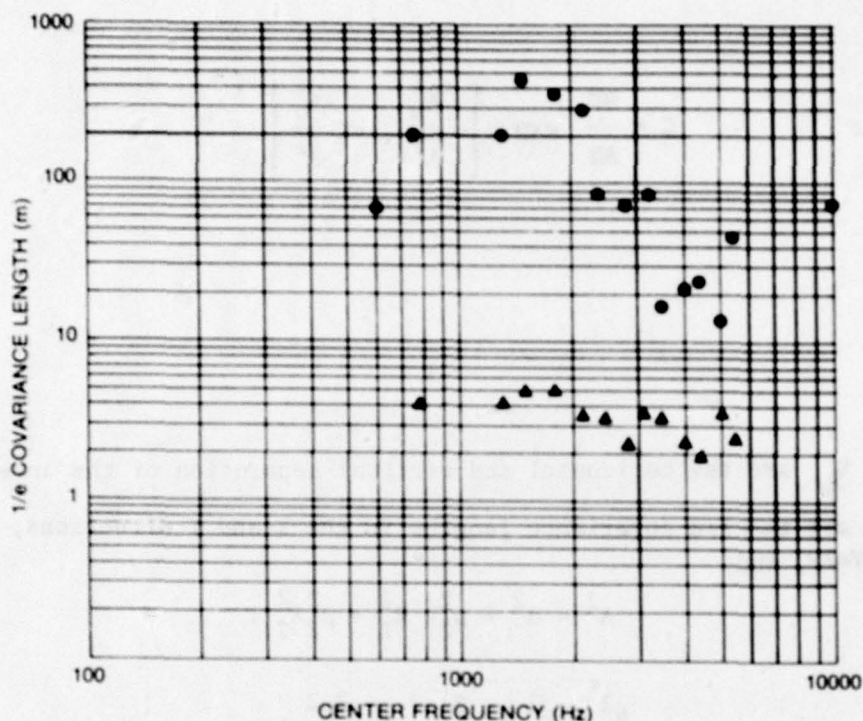


Figure 14. Spatial Separation for Covariance to Decay to $1/e$ as a Function of Pulse Center Frequency, AFAR 18-nmi Direct Path (130 ms Gaussian Envelope Pulses, 3 s Pulse Repetition Interval). The Horizontal Separation Is Shown With Dots, the Vertical Separation With Triangles

TIME LAGGED SPATIAL COVARIANCE

The covariance lengths of figure 14 were derived by crosscorrelating the outputs of two antennas at zero time lag. Since the inhomogeneities in the ocean volume are in motion, one might expect the peak covariance between two antennas to occur at nonzero time delay.^{14,15} Figure 15 shows time lagged crosscovariance functions computed between antenna pairs for the 18-nmi direct path. The (almost) horizontally separated antenna pair shows no evidence of a peak at nonzero time lag, presumably a reflection of the long horizontal covariance lengths. In contrast, the vertically separated pair shows obvious nonzero lag peaks. The dominance of vertical variation is consistent with an internal wave viewpoint as the source of time variability.¹⁶ Figure 16 shows four sets of fourteen 6-hr average lagged spatial covariance functions arranged in order of increasing vertical separation. Figure 17 shows the corresponding result for a single long term average (6 X 14 = 84 hr).

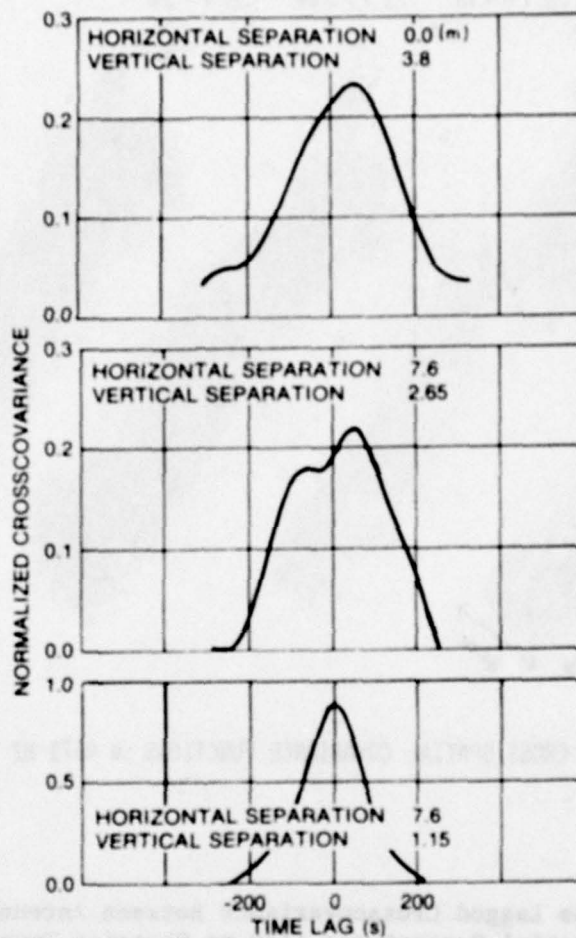
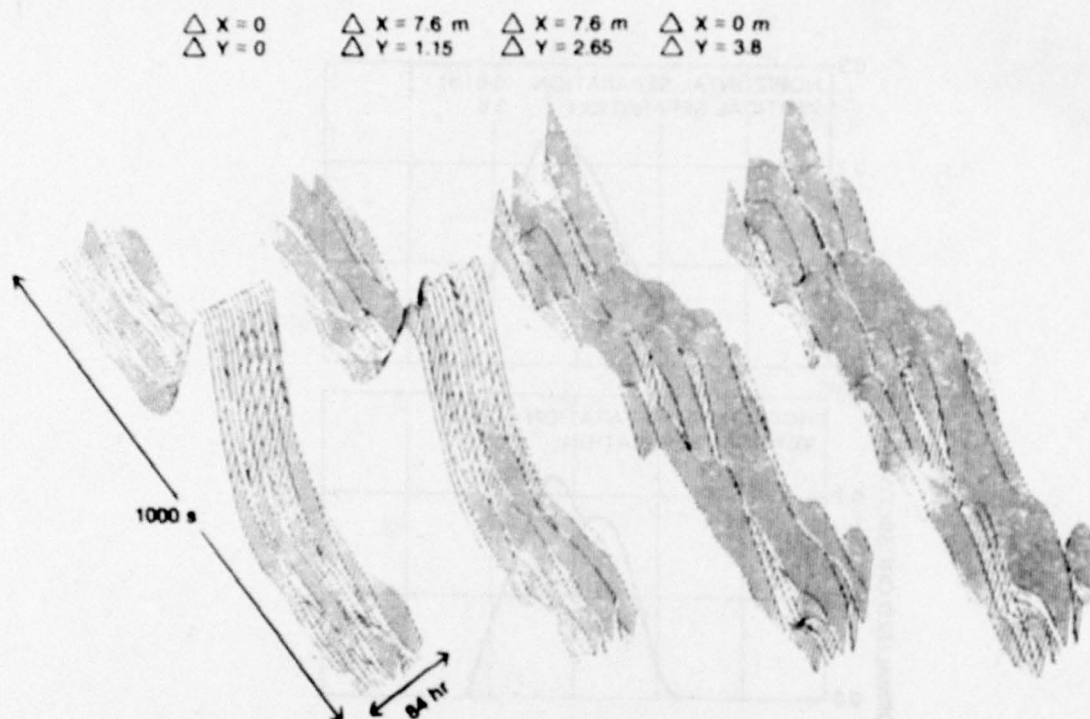


Figure 15. Time Lagged Crosscovariance Between Spatially Separated Antenna (130 ms Gaussian Envelope Pulses, 4671 Hz Center Frequency, 10.158 s Pulse Repetition Interval, 6 hr Average).
The Antenna Pairs Lie in a Plane Perpendicular to Line of Sight.



LAGGED CROSS SPATIAL COVARIANCE FUNCTIONS @ 4671 HZ

Figure 16. Time Lagged Crosscovariance Between Antenna Pairs at the Indicated Spatial Separations (130 ms Gaussian Envelope Pulses, 4671 Hz Center Frequency, 10,158 s Pulse Repetition Interval). ΔX Represents the Horizontal Separation, ΔY the Vertical Separation. Each Group Contains 14 Covariance Estimates From Contiguous Time Blocks. Each Estimate is a 6-hr Average (6 x 14 = 84 Total Data hr).

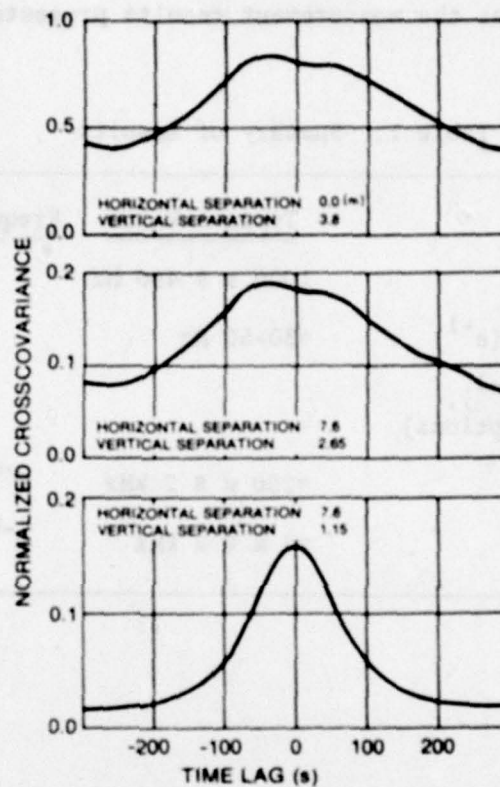


Figure 17. Time Lagged Crosscovariance Between Spatially Separated Antennas (130 ms Gaussian Envelope Pulses, 4671 Hz Center Frequency, 10.158 s Pulse Repetition Interval, 84 hr Averages). The Antennas are in a Plane Perpendicular to Line of Sight

SUMMARY

Table 1 summarizes the measurement results presented for the 18 nmi direct path.

Table 1. Summary of Results

	Typical Value	Frequency Dependence
Time Covariance (e^{-1})	1000 s @ 400 Hz	$f^{-1.1}$
Frequency Covariance (e^{-1})	≈ 30 -50 Hz	none
Spatial Covariance (e^{-1}), (Gaussian shape assumptions)		
Horizontal	≈ 200 m @ 2 kHz	$f^{-\alpha}$; $\approx 1/2 \leq \alpha \leq 1$
Vertical	≈ 4 m @ 2 kHz	$f^{-1/2}$

In addition:

1. The envelope statistics are approximately Rayleigh.
2. The variance of \log_e intensity is $\pi^2/6$ (predicted value for Rayleigh fading).
3. Time lagged spatial covariance functions reveal evidence of spatial transport due to the motion of refractive index inhomogeneities.

The results presented in this report define propagation characteristics under a very limited set of experimental conditions. Their main values are the stability of experiment geometry, the existence of detailed environmental data, and the repeatability of results. They should be useful in quantitative evaluation of theoretical propagation models. Clearly, additional experimentation is necessary under different conditions of geometry and environment. Finally, propagation between moving platforms can be expected to strongly affect measured results.

EXTRAPOLATION OF RESULTS

This section contains qualitative extrapolations of the AFAR strong fluctuation regime results to other ocean acoustic propagation conditions. The remarks are based on a combination of measured oceanographic parameters and physics reported by S. M. Flatte.¹² The AFAR strong fluctuation results presented above were for a shallow angle (≈ 2 deg), shallow depth (≈ 600 m), volume only path with fixed end-points. We make the following qualitative generalizations subject to the caveat, "... acoustic experiments invariably fall into 'anomalous' regions"¹⁶

STEEPER RAYS

When the deterministic ray path departs significantly ($>$ few degrees) from horizontal, the sound speed fluctuation correlation length along/transverse to the path decreases/increases rapidly due to the large ratio of horizontal to vertical correlation lengths in the ocean (typically $> 10:1$).

The contribution to acoustic phase fluctuation at any point along a ray path decreases with the correlation length of sound speed fluctuations measured along the ray direction at that point. Also, the number of micropaths formed by scattering of a deterministic ray decreases with increasing correlation length transverse to the ray direction.

Therefore, for a fixed path length, steeper rays have smaller rms phase fluctuation and form fewer micropaths (i.e., longer paths are required to reach the region of saturated fluctuations).

DEEPER RAYS

The variance of sound speed generally decreases with depth, resulting in smaller acoustic phase fluctuation. Longer propagation ranges are required before the phase differences in a tube of rays along a deep path are large enough to cause self-interference. Additionally, both horizontal and vertical sound speed fluctuation correlation lengths increase with depth.

GEOGRAPHIC POSITION

There are certainly large variations in oceanographic parameters with geography; however, the limited experimental data available in the literature indicate some degree of universality in spatial and temporal sound speed fluctuation spectra. Recent measurements by the AFAR group (unpublished) reveal a similarity in the depth dependence of sound speed variance for two separate regions in the North Atlantic and a third area in the Gulf of Mexico.

PLATFORM MOTION

When either or both endpoints of an acoustic link are in motion, the correlation time of an acoustic path will decrease as the translated (and rotated) path sweeps through independent regions of sound speed fluctuation. The large ratio of horizontal to vertical sound speed correlation length will result in similar ratio in the relative effects of horizontal and vertical platform speeds. Unpublished data of the AFAR group show that for platforms translating horizontally and transverse to an ocean volume acoustic path, signal correlation time falls off linearly with speed for speeds in excess of ~ 5 knots.

CONCLUSION

The information presented in this document shows that signals transmitted along acoustic paths in the ocean that contain no boundary interactions are randomly perturbed (smeared) in time, frequency, and angle. Qualitative extrapolation to other conditions of propagation is possible, and the reader who is interested in more physical insight and numerical precision is urged to read references 11, 12, 15, and 16.

REFERENCES

1. A.W. Ellinthorpe, The Azores Range, NUSC Technical Document 4551, Naval Underwater Systems Center, New London, CT, 11 April 1973.
2. J.R. Gerrebout, The AFAR Project - A Valediction, NUSC Document 3103-66-77, Naval Underwater Systems Center, New London, CT, June 1977.
3. A.W. Ellinthorpe and H. Freese, Exploitation of the Azores Fixed Acoustic Range (AFAR) Through May 1973, NUSC Technical Report 4647, Naval Underwater Systems Center, New London, CT, 2 October 1973.
4. A.W. Ellinthorpe and A.H. Krulisch, "Preliminary Account of the AFAR Microstructure Measurement Operation," NUSC Technical Memorandum No. TE-105-75, Naval Underwater Systems Center, New London, CT, 12 May 1975.
5. B.G. Buehler, "Temperature and Sound Speed Measurements Along Horizontal Towing Paths at AFAR," NUSC Technical Memorandum No. TE-27-76, Naval Underwater Systems Center, New London, CT, 1 March 1976.
6. H.A. Freese and P. Hargraves, "Towed Vertical and Horizontal Magnitude Squared Coherence of Index of Refraction Inhomogeneities Measured in the Vicinity of the Azores Fixed Acoustic Range (AFAR)," NUSC Technical Memorandum No. 3103-145-76, Naval Underwater Systems Center, New London, CT, 10 August 1976.
7. B.G. Buehler, "Spatial Power Spectral Estimates of Temperature and Sound Speed Fluctuations Along Horizontal Towing Paths at the AFAR," NUSC Technical Memorandum No. TE-38-76, Naval Underwater Systems Center, New London, CT, 12 March 1976.
8. B.G. Buehler, "Spatial Derivative and Variance Estimates of Sound Speed and Temperature Fluctuations Measured Along Horizontal Tow Paths at the AFAR," NUSC Technical Memorandum No. TE-3-76, Naval Underwater Systems Center, New London, CT, 2 January 1976.
9. H.A. Freese and P. Hargraves, "The Horizontal and Vertical Coherence of Moored Oceanic Temperature Measurements Observed at the AFAR," NUSC Technical Memorandum No. TE-56-76, Naval Underwater Systems Center, New London, CT, 13 April 1976.

10. H.A. Freese, "Signal Variability Experiments on 1.5 Nautical Mile Direct and Surface Scatter Paths Observed at the Azores Fixed Acoustic Range," NUSC Technical Memorandum No. TE-110-76, Naval Underwater Systems Center, New London, CT, June 1976.
11. V.I. Tatarski, Wave Propagation in a Turbulent Medium, McGraw-Hill, NY, 1961.
12. S.M. Flatte, ed., Sound Transmission Through a Fluctuating Ocean, Technical Report JSR-76-39, Stamford Research Institute, Menlo Park, CA, May 1977.
13. Personal Communication, A.H. Nuttall, NUSC, New London, CT.
14. B.H. Briggs et al., "The Analysis of Observations on Spaced Receivers of the Fading of Radio Signals," Proceedings of the Royal Society, Published in London, England, by the Royal Society, Physics Society, B, 63, 1950, pages 476-490.
15. R.W. Lee and J.C. Harp, "Weak Scattering in Random Media, With Applications to Remote Probing," Proceedings of the IEEE, Published in New York by the IEEE, vol. 57, no. 4, April 1969, pages 375-406.
16. W.H. Munk and F. Zachariasen, "Sound Propagation Through a Fluctuating Stratified Ocean," Journal of the Acoustical Society of America, vol. 59, no. 4, April 1976, pages 818-838.

INITIAL DISTRIBUTION LIST

Addressee	No. of Copies
NSEA (SEA 633Y) J. Calabrese	1
(SEA 63D)	1
NORDA (Code 110) Dr. R. Goodman	1
(Code 486) Dr. H. Bezdek	1
ONR (Code 222)	1
(Code 220T)	1
NAVELEX (PME 124) CAPT H. Cox	1
(Code 320)	1
OASN (RE&S)	2
NAVPGSCOL (Dr. H. Medwin)	1
NRL (Code 120A) Dr. W. Moseley	1
NOSC (Code 7123) D. E. Marsh	1
CNO (Op 981G)	1
NAVOCEANO	1
NSEA (SEA 996) Tech Library	1
DDC	12